Restoration of an image degraded by vibrations using only a single frame

Yitzhak Yitzhaky, MEMBER SPIE
G. Boshusha
Y. Levy
Norman S. Kopeika, MEMBER SPIE
Ben-Gurion University of the Negev
Department of Electrical and Computer
   Engineering
P.O. Box 653
Beer Sheva, 84105 Israel
E-mail: itzik@eesrv.bgu.ac.il
      kopeika@bguee.bgu.ac.il

Abstract. A recently developed method for the restoration of motion-blurred images is investigated and implemented for the special complicated case of image blur due to sinusoidal vibrations. Sinusoidal vibrations are analyzed in the context of blur identification and image restoration. The extent of the blur and the optical transfer function (OTF) are identified from the blurred image by a straightforward process without the use of iterative techniques. The blurred image is restored using a simple Wiener filter with the identified OTF. The main novel achievement is the use of only a single vibrated blurred image as input information, on which the restoration process is based. The various cases of blur types that depend on the imaging conditions are considered. Examples of blur identification and image restoration are presented. © *2000 Society of Photo-Optical Instrumentation Engineers.* [S0091-3286(00)01408-2]

1 Introduction

Mechanical vibrations characterized by sinusoidal motion exist primarily in imaging systems that include circular motion such as that of an engine. This is common in cases such as airborne or vehicular imaging systems. In such cases, the vibrations often limit the image resolution and target acquisition.

A common model for motion-blurred image formation is a linear, space-invariant blur effect. Such a model is practical and usually satisfying. Simple filters used to restore blurred images require knowledge of the blur function represented by the point spread function (PSF) or its Fourier transform, the optical transfer function[1,2] (OTF). If the motion (temporal) function is known *a priori* or can be physically measured by a motion sensor, it can be used to calculate the blur function.[2,3] However, such information is usually not available. When consecutive frames of a video signal are available, a method to identify the blur caused by vibrations was developed.[4] The drawback is that knowledge about specific characteristics in the image is required. Here, we consider image restoration of a single image, without any knowledge or measurement of the function of motion. Vibrational motion blur is an especially difficult problem and an especially important one to solve.

Wide research during the last four decades considered the problem of restoration of images blurred by motion where only a single image is given and the blur function is not known *a priori*. Almost all of these researches modeled the motion during exposure as uniform velocity.[5–9] The justification for such a model is that in various situations, the motion does not change much during the short exposure time (in real-time imaging, about 1/30 s). When uniform velocity motion is assumed, the blur identification process requires an approximation of only two parameters that completely determines the blur: its extent and the direction in the image. When the image is truly blurred by a uniform velocity motion, it is relatively easy to identify these parameters from the image.[5,10] The problem with such an assumption is that it is not true in many practical situations such as vibrations. Although vibrations are a common problem in imaging systems, it is rarely considered in the literature in the context of blur identification and image restoration from an image. The reason is probably the complicated and random nature of the vibrations MTF (Refs. 2, 3, 11, and 12).

A new method recently developed[10,13] called the ''whitening method'' performs direct numerical identification of the blur function resulting from motion. Compared to other direct blur identification methods, this method showed better identification performance.[14] However, it was examined only for the cases of uniform velocity motion and accelerated velocity motion. Here, we use this method to deal with the more complicated and common problem of image blur caused by vibrations, when the motion function is unknown and only a single blurred image is given. Both high- and low-frequency vibrations are considered.

A short analysis of sinusoidal motion blur, presenting its various appearances, is presented in Sec. 2. The principles of the blur identification method are presented in Sec. 3. Section 4 shows the implementation and analysis of vibration blur identification, considering the various cases of vibrations blur and its application to image restoration. Summary and conclusions appear in Sec. 5.

2 Sinusoidal Motion Blur

In a periodic sinusoidal motion, the relative motion between the camera and the photographed object is

$$x(t) = D \cos 2\pi t/T_0, \tag{1}$$
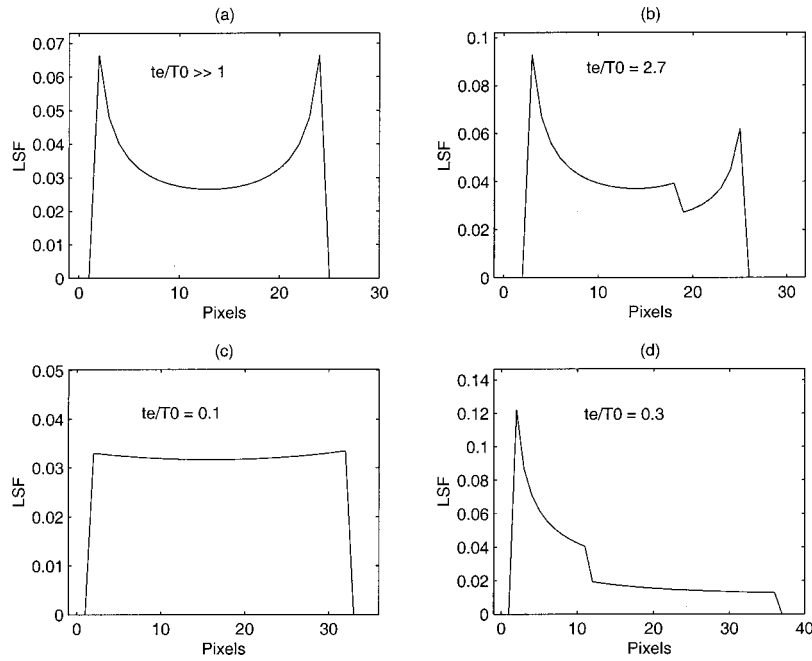
Fig. 1 Different LSF types considered with sinusoidal vibrations: (a) high-frequency vibrations, where the exposure time is much longer than the vibration period; (b) high-frequency vibrations, where the exposure time is not much longer than the vibration period; (c) low-frequency vibrations, where motion direction does not change during the exposure time; and (d) low-frequency vibrations, where motion direction does change (forward and backward) during exposure time.

where D is the amplitude of the sinusoidal displacement and T_0 is its period.

From an imaging aspect, sinusoidal vibrations are divided into two types according to the relation between the exposure time t_e and the sinusoidal vibration temporal period. Vibrations are considered high frequency when the vibration period is smaller than the exposure time, and as low frequency when the vibration period is larger than the exposure time.[2,3] For a given vibration amplitude, the high-frequency-vibration OTF is known. It is a closed-form expression based on the fact that the blur extent is the peak-to peak sine wave displacement. However, the low-frequency-vibration OTF is random. Since it depends on the random instant during the vibration period wherein the exposure begins, the actual MTF is one of many possibilities that can be much different from each other.[2,3,11] For high-frequency vibrations ($t_e \gg T_0$) the line spread function (LSF) can be approximated by[2,3]:

$$\text{LSF}_{\text{HF}}(x) = \frac{1}{\pi(D^2 - x^2)^{1/2}}, \quad |x| < D, \tag{2}$$

where x is the spatial coordinate. Equation (2) is an accurate description of the LSF when $t_e = nT_0$, where n is a natural number. The OTF for this case is given by the Fourier transform of Eq. (2). The absolute value of the OTF is the MTF[2]:

$$\text{MTF}_{\text{HF}}(u) = J_0(2\pi u D), \tag{3}$$

where J_0 is zero-order Bessel function, and u is the spatial frequency coordinate. The total blur extent for the high-vibration-frequency case is the peak-to-peak displacement, which is $2D$. The LSF in this case can completely be determined by the blur extent. Figures 1(a)–1(d) present some different LSF types considered with sinusoidal vibrations. The case of high frequency is shown in Fig. 1(a). When the exposure time is a little longer than the vibration period, although the total blur extent is the same, the shape of the LSF is different. An example of such a case appears in Fig. 1(b). In both cases the vibration amplitude is 30 pixels.

The case of low vibration frequency involves time exposures shorter than the vibration period. In this case, the blur function resulting from the motion is random and depends on the specific time in which exposure takes place during the vibration period. Since the motion in this case is a random portion of the sinusoidal vibration, the LSF of this motion is a random portion of the LSF described in Eq. (2). The relation between the blur extent and the vibration amplitude is linear. However, nonlinear relations exist between the blur extent and the other vibration parameters (the vibration period time, the exposure time, and the beginning instance of exposure during vibration period). Detailed analysis and formulation of these relations appear in Ref. 11. Here, these relations are presented mainly qualitatively. For a given vibration amplitude, period, and exposure time, the blur extent of a low-frequency-vibration case is limited according to[2,11]:

$$D\left[1 - \cos\left(\frac{2\pi}{T_0}\right)\left(\frac{t_e}{2}\right)\right] \leq d_{\text{LF}} \leq 2D\sin\left[\left(\frac{2\pi}{T_0}\right)\left(\frac{t_e}{2}\right)\right]. \tag{4}$$

This blur extent is obviously smaller than the total $2D$ extent of that resulting from the complete vibration. However, in real-life situations the vibration amplitude in the low-frequency motion case is in many cases much greater than that of the high-frequency motion case. Figure 1 shows examples of four different LSFs resulting from vibrations. Figures 1(a) and 1(b) show examples of high-frequency-vibration LSFs where the vibration amplitude is 12 pixels. The difference between these two examples is the relation between the exposure time and the vibration period (t_e/T_0). In Fig. 1(a), the exposure time is n times the vibration period, where n is an integer [Eq. (2)], and in Fig. 1(b) the exposure time is 2.7 times the vibration period. Figures 1(c) and 1(d) show examples of low-frequency-vibration LSFs where the vibration amplitude is 50 pixels. The difference between these two examples is the relation (t_e/T_0) and the beginning time of the exposure during the vibration period. In the case of Fig. 1(c), t_e/T_0 is 0.1 and the motion direction does not change during the exposure time, while in the case of Fig. 1(d), t_e/T_0 is 0.3 and the motion direction does change (forward and backward) during this time. Although the exposure time in Fig. 1(d) is three times greater than in Fig. 1(c), the blur extents created in both cases are very close [31 pixels in Fig. 1(c) versus 35 pixels in Fig. 1(d)]. The reason is that the average of motion velocity in the case of Fig. 1(d) is about three times smaller. In the LSF of Fig. 1(d), there is a knee at the 10th pixel. A knee in the LSF appears when forward and reverse movements of different lengths occur during the exposure. For a better description of the LSF in this case, we determine a second blur extent that ends at the location of the knee [from the 1st pixel through the 10th in Fig. 1(d)]. The effect of this knee is discussed later.

3 Blur Identification Method

A recently developed[10,13] blur identification method is implemented here for the identification of the blur caused by vibrations. The method is performed in a straightforward manner without iterations and it uses as input information the blurred image only. The PSF of the blur is first identified and then used to restore the blurred image. This method has shown a powerful ability to identify motion blur from an image when compared to other straightforward methods.[14]

The blur identification here is based on the concept that image correlation characteristics along the direction of motion are affected mostly by the blur and are different from the characteristics in other directions. By filtering the blurred image we emphasize the PSF correlation properties at the expense of those of the original image. For this purpose a pseudo-image-whitening filter is implemented in the motion direction and perpendicular to it. A simple high-pass filter can be used for this purpose. Prior to this operation, the motion direction is identified by measuring the direction where the image resolution is maximally decreased. Both PSF parameters (extent and direction) and a PSF approximation are identified by this method.

After identifying the motion direction in the image, a high-pass (whitening) filter is implemented in the motion direction and perpendicular to it. Implementation of such a filter will form patterns similar to the high-pass-filtered

PSF, surrounded by extremely suppressed de-correlated regions. The filtered image in the Fourier domain $\Delta G(u,v)$ can then be formulated as

$$\Delta G(u,v) = G(u,v)W(v)W(u), \qquad (5)$$

where $W(v)$ and $W(u)$ are the pseudowhitening filters perpendicular to and in the motion direction that coincide with the frequency u axis. These patterns can be evaluated by performing an autocorrelation operation to all the filtered image lines in the motion direction, and then averaging them. Such operation also suppresses the noise stimulated by the whitening operations and causes cancellation of correlation properties left over from the original image that can be different from one line to another. For many motion blur cases, the blur extent is the distance between the center of the average autocorrelation and its global minimum.[10]

Since the average autocorrelation function is usually similar to the autocorrelation of the filtered PSF, the discrete Fourier transform of the average autocorrelation $\bar{S}_{\Delta G}$ is also similar to the power spectrum of the filtered PSF, i.e.,

$$\bar{S}_{\Delta G} \approx S_{\Delta \mathrm{PSF}}, \qquad (6)$$

where $S_{\Delta \mathrm{PSF}}(u) = |H(u) \cdot W(u)|^2$ and $H(u)$ is the Fourier transform of the PSF, which is actually the OTF of the motion blurring system.[1,2] The MTF of the blur is the absolute value[1,2] of the OTF, and can be approximated from Eq. (6) by[13]

$$\mathrm{MTF}(u) \approx \frac{[S_{\Delta G}(u)]^{1/2}}{|W(u)|}. \qquad (7)$$

The PTF can be calculated from the MTF by[15]:

$$\mathrm{PTF}(u) = -\frac{1}{2\pi} \int_0^{2\pi} \ln\{\mathrm{MTF}(\alpha)\} \cot\frac{u-\alpha}{2} \, d\alpha. \qquad (8)$$

Equation (8) for the calculation of the PTF requires the condition that the PSF is a minimum phase function, i.e., a real, causal, and stable PSF. The OTF used to restore the blurred image is obtained by[2]:

$$H = \mathrm{MTF} \exp(j\mathrm{PTF}). \qquad (9)$$

The PSF is then obtained by inverse Fourier transforming the identified OTF.[2]

4 Identification of the Blur Caused by Vibrations

This section is divided into two parts: identification of the blur extent, and identification of the blur function. First, this division is explained. To achieve optimal restoration of the blurred image, the complete description of the blur, which is its PSF, should be known. The goal of this work is to identify this information from the blurred image. However, it is very hard to achieve a given reliable complete
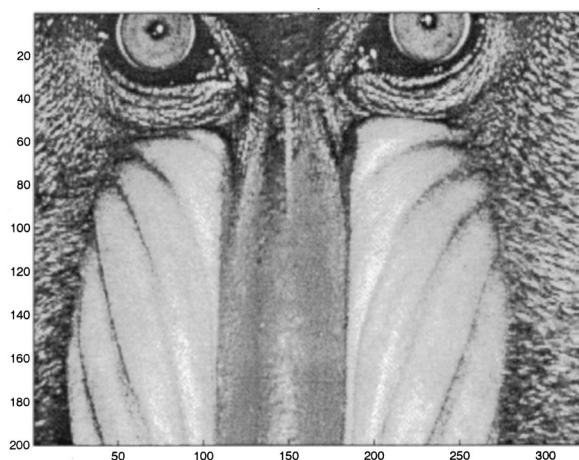
Fig. 2 Original unblurred image.

PSF from the blurred image. The blur extent in the image is partial information that can be used to approximate the PSF. During the last 4 decades, almost all of the research in motion blur identification from an image considered only blur extent identification. In certain situations there is knowledge about the amplitude and frequency of the vibrations, and the exposure time is usually known. In such cases, identification of the blur extent can lead to a good approximation of the PSF.

4.1 Identification of the Blur Extent

4.1.1 High-frequency vibrations

In this case, the original unblurred image presented in Fig. 2 was blurred according to the high-frequency-vibration LSF described by Eq. (2) with blur extents varying from 2 to 160 pixels. The results of the blur extent identification

are plotted in Fig. 3 for two values of SNR: 30 and 25 dB. It can be seen that for a 30-dB SNR all the blur extents are perfectly identified. However, for 25-dB SNR, a correct identification was achieved only for blur extents from 0 to 43 pixels, and after that some errors appear as blur extent increases. The reason is that as the blur extent increases, the autocorrelation of the filtered blurred image expressed by its Fourier transform $\bar{S}_{\Delta G}$ is less affected by the correlation properties of the PSF because fewer PSF patterns can fit into the blurred image. Therefore, $\bar{S}_{\Delta G}$ is more affected by the noise, the similarity expressed in Eq. (6) is decreased, and so is the blur extent identification capability.

4.1.2 Low-frequency vibrations

The shape of the PSF in this case depends on the random instant the exposure begins during the vibration period (t_x) and the relation between the exposure time and the vibration period (t_e/T_0). Therefore, to examine the blur extent identification capability for the various motion portions in a vibration, the extents of vibration blurs were identified for different values of t_e/T_0, each, for different values of t_x changing with small increments throughout the vibration period. In each situation, the blur extent identified from the image was compared to the true one. Examples of true blur extent versus that identified appear in Figs. 4–7. The vibration amplitude was 50 pixels and a normally distributed zero mean white noise forming a 40-dB SNR was added. In each figure, the empty diamonds show the total extent of the true LSF and the empty squares show the second (smaller) true blur extent starting from the knee if it exists. In most of the cases [such as the example in Fig. 1(c)], a second blur extent does not exist and therefore is represented by a square located on the horizontal zero axis. When a knee does appear in the LSF [such as the example in Fig. 1(d)], the second blur extent starting from that knee
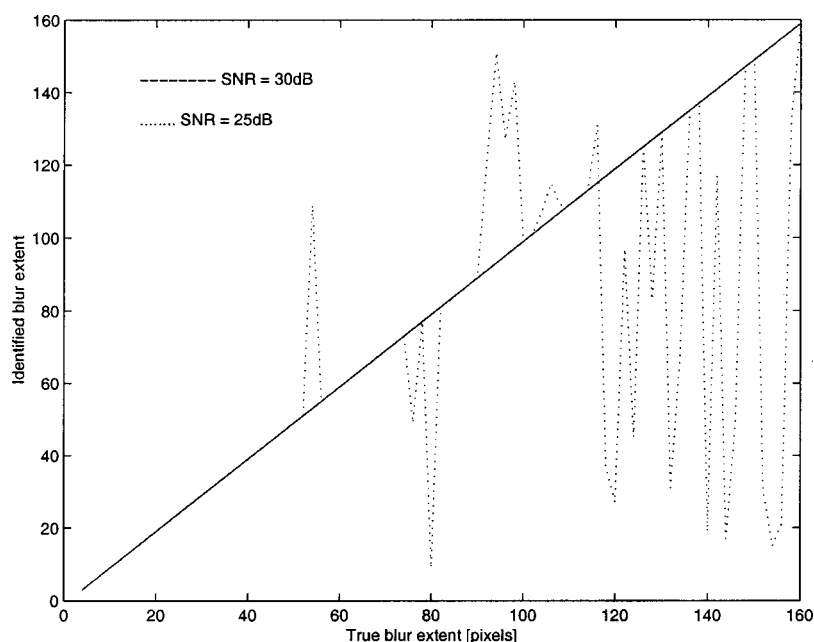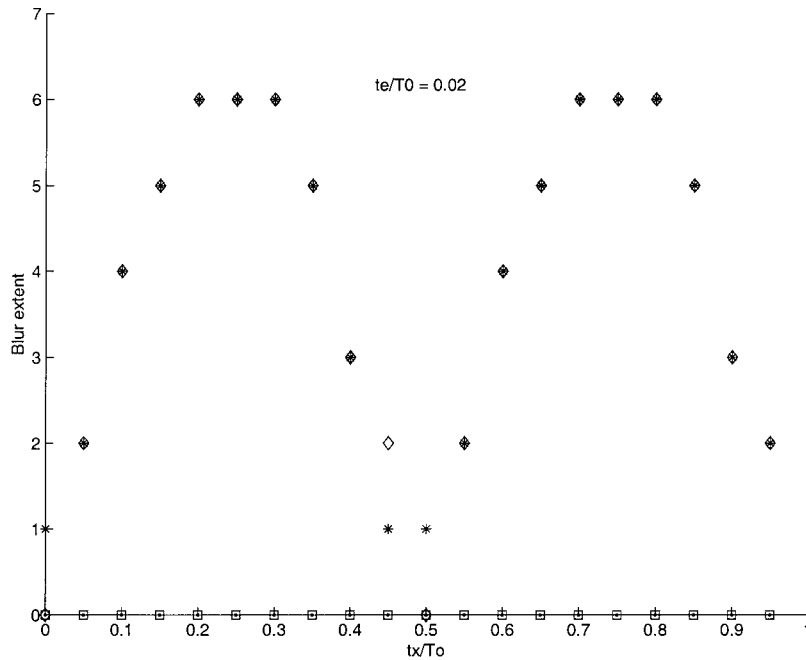

Fig. 3 Blur extent identification results for high-frequency horizontal vibration blurs, extending from 2 to 160 pixels. The image size is 320×200 pixels.

Fig. 4 True blur extents represented by empty diamonds and squares, versus identified blur extents represented by stars and points. The imaging parameters are: vibration amplitude is 50 pixels, $t_e/T_0 = 0.02$, and SNR=40 dB.

is represented by a square located above the horizontal zero axis. The blur extents identified from the blurred image are represented by the stars and the points. When a knee does not exist in the LSF, the stars represent the identified LSF extent. When a knee does exist in the LSF, the stars represent the identified second extent starting from the knee, and the points represent the total LSF extent. We can see from the graphs that almost all of the blur extents are perfectly identified from the image (when a star or a point is located inside a diamond or a square). We can also see that a knee in the LSF exists only when the exposure time is not much smaller than the vibration period.

When the noise is increased to 35 dB, few blur extent identification mistakes occur for the higher values of t_e/T_0. Few more identification mistakes appear when the noise is increased to 30 dB. However, as the relation t_e/T_0 is smaller, the identification is less sensitive to noise. For
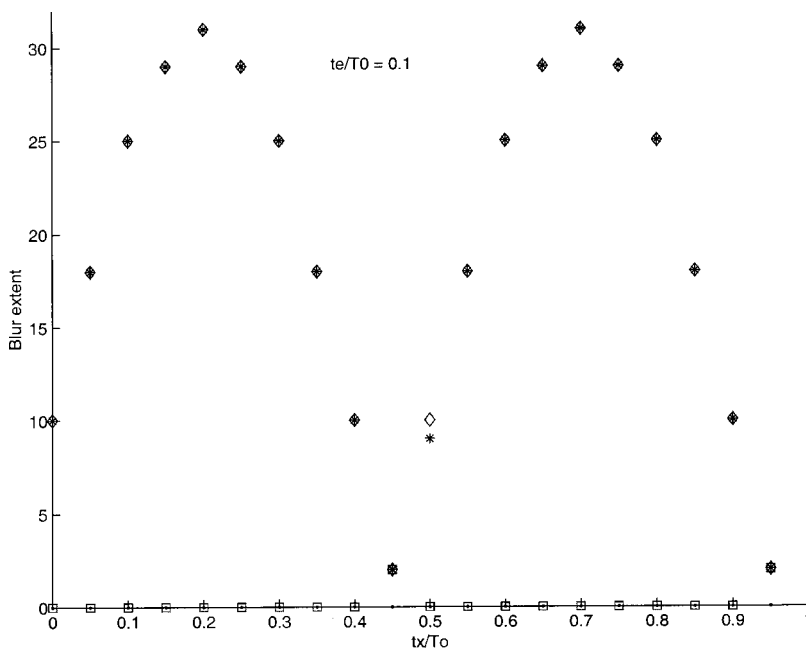
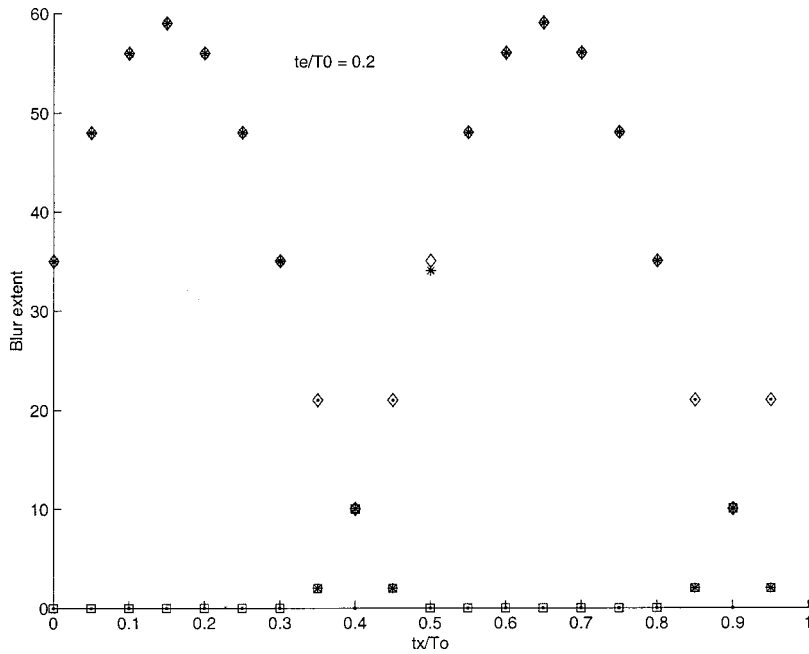**Fig. 5** Same as Fig. 4, but with $t_e/T_0 = 0.1$.

Fig. 6 Same as Fig. 4, but with $t_e/T_0=0.2$.

the case of $t_e/T_0=0.02$, the blur identification results for 20 dB SNR are the same as for 40 dB SNR (Fig. 4).

4.2 Identification of the Blur Function and Image Restoration

The blur function is expressed here by the MTF and the PTF, which form the OTF [Eq. (9)] that is the Fourier transform of the PSF. These quantities express the properties of the blurring process as a function of the spatial frequency and therefore give a profound description of its effect on the image.[2] Figure 8 shows an example of blur

identification and image restoration results for a case of high frequency vibration blur. The original image as it appears in Fig. 2 was degraded by a high-frequency-vibration blur with 24-pixel blur extent [as shown in Fig. 1(a)] and 30-dB SNR. The identified MTF and PTF were obtained using Eqs. (7) and (8), respectively. As a result of a non-ideal MTF identification, the identified PTF is usually shifted with regard to the true one. Therefore, the PTF was normalized to be zero at the point of zero frequency. Otherwise, a shift of gray-level values would be observed in the restored image. Figures 8(c) and 8(d) present the iden-
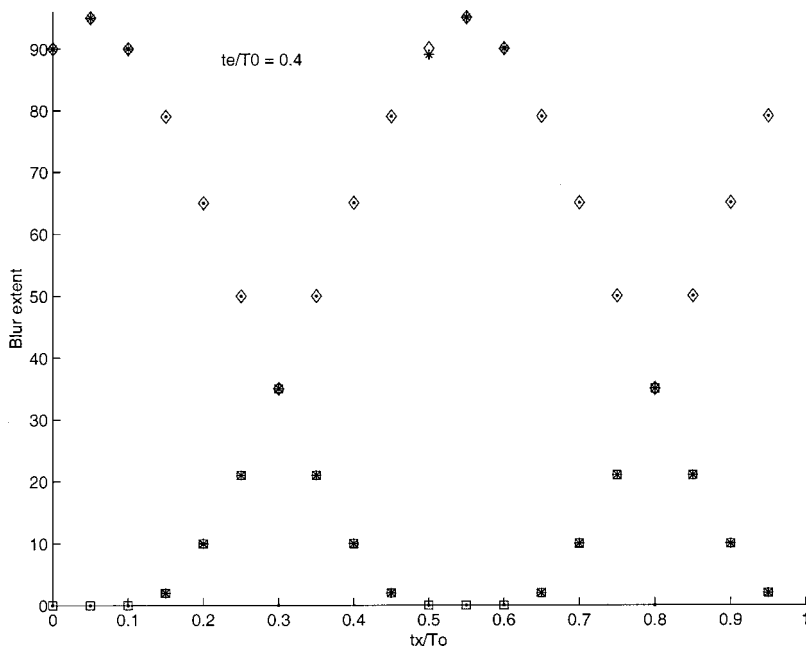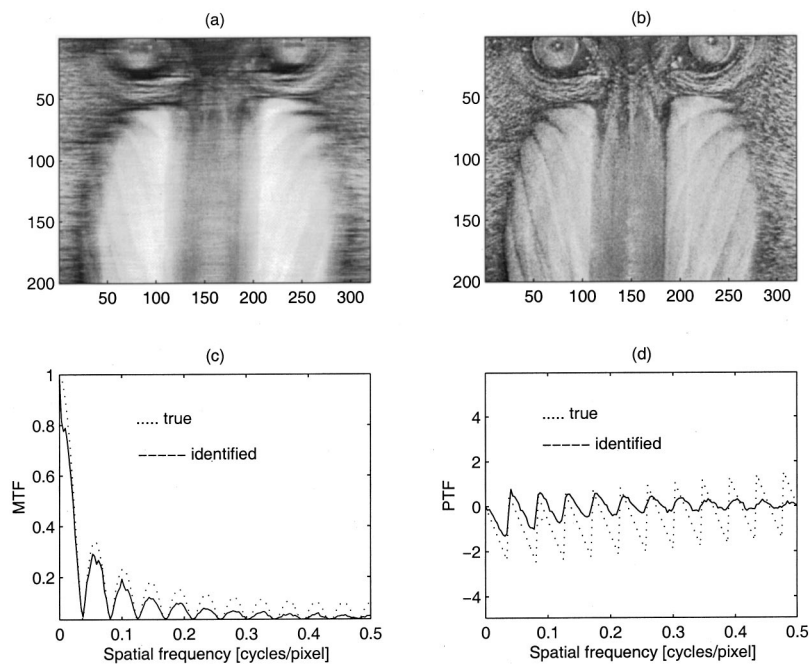

Fig. 7 Same as Fig. 4, but with $t_e/T_0=0.4$.

Fig. 8 Results of blur identification and image restoration: (a) image degraded by high-frequency-vibration blur with 24-pixel blur extent and 30-dB SNR, (b) the restored image using the identified blur function, (c) the true MTF versus the identified MTF, and (d) the true PTF versus the identified PTF.

tified versus the true MTF and PTF, respectively. The restored image appears in Fig. 8(b) and was obtained using a simplified Wiener filter using the OTF that is calculated in Eq. (9). The restoration result can be evaluated by comparing it to the blurred version in Fig. 8(a) relative to the ideal image in Fig. 2, which would be obtained approximately if the image would be restored with the true OTF.

The quality of the improved image and its resemblance to the original image depend directly on how similar the identified blur function is to the true one. For a 30-dB SNR, successful blur identification and image restoration can be obtained for horizontal blurs of high-frequency vibration with extents up to half the image size. However, as the noise increases, the similarity between the identified and the true blur decreases, as with the blur extent identification shown in Fig. 3.
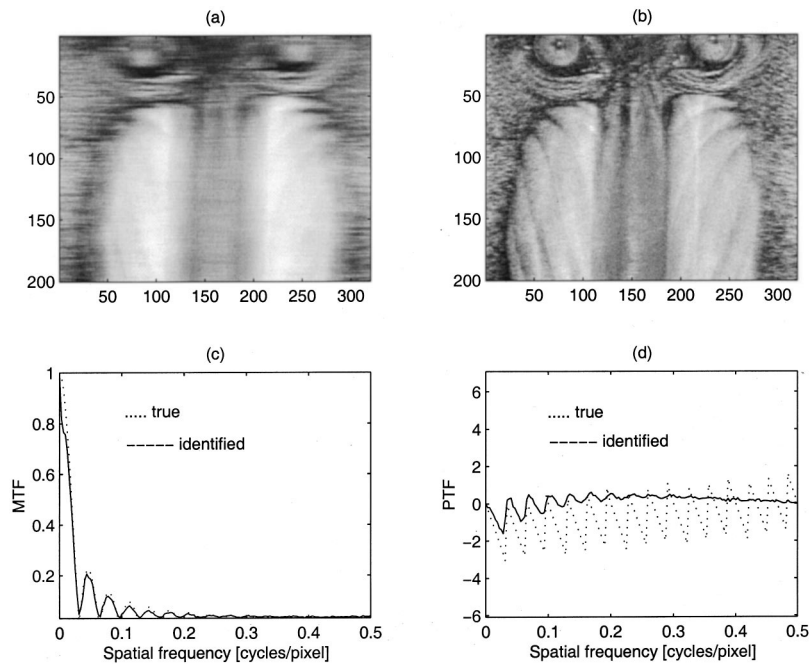
Examples of blur identification and image restoration for cases of low-frequency vibrations are presented in Figs. 9–11. In all examples, the image was degraded by a portion of a vibration period with a 50-pixel amplitude and an additive noise forming a 30-dB SNR. In Figs. 9 and 10 the relation t_e/T_0 is 0.1, but the difference between them is the instant during the vibration period where the exposure starts. In Fig. 9, this instant is at the beginning of the cosine vibration period ($t_x=0$), forming a 10-pixel blur extent. In Fig. 10, the exposure starts at $0.2T_0$, forming a 31-pixel blur extent, as shown in Fig. 2(c). In Fig. 11, the relation t_e/T_0 is 0.3 and t_x is $0.4T_0$. Such conditions cause a knee in the LSF forming a total of 35 pixel blur extent and a second extent of 10 pixels ending at the knee. The PSF created in this case is shown in Fig. 2(d).

In the case of low-frequency blur, improvement of the degraded image can be achieved for blurs up to half the

image size. However, the quality of the restored image decreases slowly as the blur size increases.

5 Summary and Conclusions

This paper deals with the problem of image motion blur caused by sinusoidal vibrations. Given only the single vibrated image, identification of the motion blur and restoration of the image using the identified results were performed. Properties of the blur such as its shape and extent are dependent on the relations between the exposure time, the vibration period, and the beginning exposure time during the vibration period. These properties were examined here in the context of blur identification. In the case of high-frequency vibrations, where the exposure time is long relative to the vibration period, reliable identification of the blur extent and a good approximation of the blur function can be achieved for SNRs higher than 30 dB. In the case of low-frequency vibrations, where the exposure time is short relative to the vibration period, two possible situations were observed and considered. One is a continuous LSF, where motion during exposure is in one direction, and the other is a noncontinuous LSF, where motion changes its direction during the exposure, which gives rise to a knee in the LSF. In the noncontinuous case, both the total LSF extent and the blur extent starting at the knee were identified from the blurred image. Identification of the blur function in the low-frequency case and restoration of the image were performed also for much different blur situations including continuous and noncontinuous PSF cases.

Fig. 9 Results of blur identification and image restoration: (a) image degraded by low-frequency-vibration blur with 50-pixel amplitude, $t_e / T_0 = 0.1$, $t_x = 0.2 T_0$, and SNR=30 dB; (b) the restored image using the identified blur function; (c) the true MTF versus the identified MTF, and (d) the true PTF versus the identified PTF.
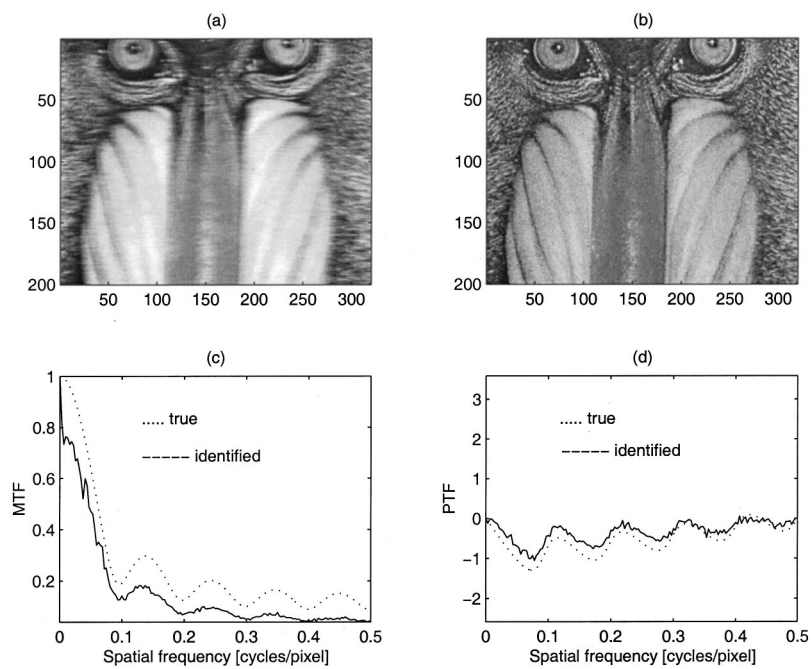
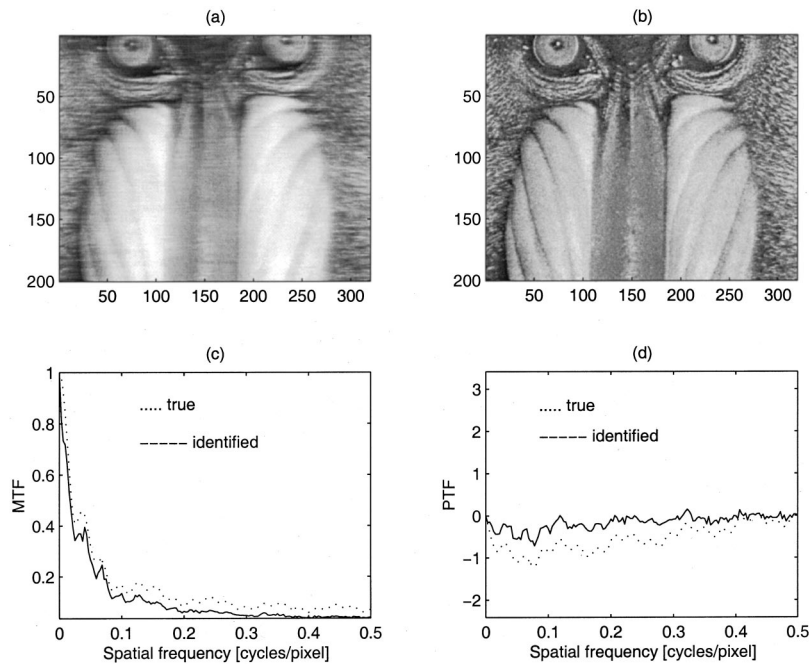**Fig. 10** Same as Fig. 9, but with $t_x = 0$.

Fig. 11 Same as Fig. 9, but with $t_e/T_0 = 0.3$ and $t_x = 0.4T_0$ forming an LSF with a knee.

References

1. A. K. Jain, *Fundamentals of Digital Image Processing*, Prentice-Hall, Englewood Cliffs, NJ (1989).
2. N. S. Kopeika, *A System Engineering Approach to Imaging*, SPIE Press, Bellingham, WA (1998).
3. O. Hadar, I. Dror, and N. S. Kopeika, ''Image resolution limits resulting from mechanical vibrations. Part IV: real-time numerical calculation of optical transfer function and experimental verification,'' *Opt. Eng.* **33**(2), 566–578 (1994).
4. O. Hadar, M. Robbins, Y. Novogrozky, and D. Kaplan, ''Image motion restoration from a sequence of images,'' *Opt. Eng.* **33**(10), 2898–2904 (1996).
5. M. Cannon, ''Blind deconvolution of spatially invariant image blurs with phase,'' *IEEE Trans. Acoust., Speech, Signal Process.* **ASSP-24**(1), 58–63 (1976).
6. R. L. Lagendijk, A. M. Tekalp, and J. Biemond, ''Maximum likelihood image and blur identification: a unifying approach,'' *Opt. Eng.* **29**(5), 422–435 (1990).
7. A. K. Katsaggelos, Ed., *Digital Image Restoration*, Springer-Verlag, New York (1991).
8. G. Pavlovic and A. M. Tekalp, ''Maximum likelihood parametric blur identification based on a continuous spatial domain model,'' *IEEE Trans. Image Process.* **1**(4), 496–504 (1992).
9. A. E. Savakis and H. J. Trussell, ''Blur identification by residual spectral matching,'' *IEEE Trans. Image Process.* **2**(2), 141–151 (1993).
10. Y. Yitzhaky and N. S. Kopeika, ''Identification of blur parameters from motion blurred images,'' *Comput. Vis. Graph. Image Process.* **59**(5), 321–332 (1997).
11. D. Wulich and N. S. Kopeika, ''Image resolution limits resulting from mechanical vibrations,'' *Opt. Eng.* **26**(6), 529–533 (1987).
12. S. Rudoler, O. Hadar, M. Fisher, and N. S. Kopeika, ''Image resolution limits resulting from mechanical vibrations. Part IV: experiment,'' *Opt. Eng.* **30**(5), 577–589 (1991).
13. Y. Yitzhaky, I. Mor, A. Lantzman, and N. S. Kopeika, ''A direct method for restoration of motion blurred images,'' *J. Opt. Soc. Am. A* **15**(6), 1512–1519 (1998).
14. Y. Yitzhaky and N. S. Kopeika, ''Comparison of direct blind deconvolution methods for motion-blurred images,'' *Appl. Opt.* **38**(20), 4325–4332 (1999).
15. M. Kunt, *Digital Signal Processing*, Chap. 7, Artech House, Norwood, MA (1986).

Yitzhak Yitzhaky received his BSc and MSc degrees in electrical and computer engineering from Ben-Gurion University of the Negev, Israel, in 1993 and 1995, respectively. He is presently a PhD research assistant and student in the electro-optics and image processing program at the same university. His current research interests are in restoration of images blurred by motion and atmosphere. Dr. Yitzhaky is a member of SPIE.

Norman S. Kopeika received the BS, MS, and PhD degrees in electrical engineering from the University of Pennsylvania, Philadelphia, in 1966, 1968, and 1972, respectively. In 1973 he joined the Department of Electrical Engineering, Ben-Gurion University of the Negev, Beer-Sheva, Israel, where he is currently a professor and incumbent of the Reuben and Frances Feinberg Chair in Electrooptics. During 1978 and 1979 he was a visiting associate professor in the Department of Electrical Engineering, University of Delaware, Newark. His current research interests include atmospheric optics, effects of surface phenomena on optoelectric device properties, optical communication, electronic properties of plasmas, laser breakdown of gases, the optogalvanic effect, electromagnetic-wave-plasma interaction in various portions of the electromagnetic (EM) spectrum, and utilization of such phenomena in EM-wave detectors and photopreionization lasers. He has published over 120 reviewed journal papers in these areas. From 1989 to 1993 he served two terms as department chair. Dr. Kopeika is a senior member of the IEEE and a member of SPIE, the Optical Society of America, and the Laser and Electrooptics Society of Israel.

Biographies of the other authors not available.